DEVELOPMENTAL DYNAMICS 234:1034–1045, 2005

Expression and Functional Analysis of Genes Deregulated in Mouse Placental Overgrowth Models: *Car2* and *Ncam1*

Umashankar Singh,[1] Tong Sun,[1] Wei Shi,[1] Ralph Schulz,[2] Ulrike A. Nuber,[2] Aikaterini Varanou,[3] Myriam C. Hemberger,[3] Rosemary W. Elliott,[4] Hiroshi Ohta,[5] Teruhiko Wakayama,[5] and Reinald Fundele[1,2]*

Different causes, such as maternal diabetes, cloning by nuclear transfer, interspecific hybridization, and deletion of some genes such as *Esx1*, *Ipl*, or *Cdkn1c*, may underlie placental overgrowth. In a previous study, we carried out comparative gene expression analysis in three models of placental hyperplasias, cloning, interspecies hybridization (IHPD), and *Esx1* deletion. This study identified a large number of genes that exhibited differential expression between normal and enlarged placentas; however, it remained unclear how altered expression of any specific gene was related to any specific placental phenotype. In the present study, we focused on two genes, *Car2* and *Ncam1*, which both exhibited increased expression in interspecies and cloned hyperplastic placentas. Apart from a detailed expression analysis of both genes during normal murine placentation, we also assessed morphology of placentas that were null for *Car2* or *Ncam1*. Finally, we attempted to rescue placental hyperplasia in a congenic model of IHPD by decreasing transcript levels of *Car2* or *Ncam1*. In situ analysis showed that both genes are expressed mainly in the spongiotrophoblast, however, expression patterns exhibited significant variability during development. Contrary to expectations, homozygous deletion of either *Car2* or *Ncam1* did not result in placental phenotypes. However, expression analysis of *Car3* and *Ncam2*, which can take over the function of *Car2* and *Ncam1*, respectively, indicated a possible rescue mechanism, as *Car3* and *Ncam2* were expressed in spongiotrophoblast of *Car2* and *Ncam1* mutant placentas. On the other hand, downregulation of either *Car2* or *Ncam1* did not rescue any of the placental phenotypes of AT24 placentas, a congenic model for interspecies hybrid placentas. This strongly suggested that altered expression of *Car2* and *Ncam1* is a downstream event in placental hyperplasia. *Developmental Dynamics 234:1034–1045, 2005.*

Key words: *Car2*; *Ncam1*; placental growth; functional redundancy

Received 13 June 2005; Revised 2 August 2005; Accepted 26 August 2005

INTRODUCTION

A functional and healthy placenta is an essential prerequisite for the development of all eutherian mammals. Thus, placental defects that severely compromise placental function generally lead to decreased fetal growth and even death (for review, see Rossant and Cross, 2001). In recent years, studies of mouse mutants produced by targeted deletion of genes involved in

The Supplementary Material referred to in this article can be found at http://www.interscience.wiley.com/jpages/1058-8388/suppmat
[1]Department of Development and Genetics, Evolutionary Biology Center, Uppsala University, Uppsala, Sweden
[2]Department of Human Molecular Genetics, Max-Planck-Institute for Molecular Genetics, Berlin, Germany
[3]Laboratory of Developmental Genetics and Imprinting, Babraham Institute, Babraham, Cambridge, United Kingdom
[4]Department of Molecular and Cellular Biology, Roswell Park Cancer Institute, Buffalo, New York
[5]Laboratory for Genomic Reprogramming, RIKEN Center for Developmental Biology, Kobe, Japan
Grant sponsor: Swedish Research Council (Vetenskapsrådet); Grant sponsor: Wallenberg Consortium North; Grant sponsor: NIH; Grant number: GM33160; Grant sponsor: Max-Planck Gesellschaft.
***Correspondence to: Prof. Reinald Fundele, Department of Development and Genetics, Evolutionary Biology Center, Uppsala University, 18A, Norbyvagen, SE-752 36, Sweden. E-mail: reinald.fundele@ebc.uu.se**

DOI 10.1002/dvdy.20597
Published online 24 October 2005 in Wiley InterScience (www.interscience.wiley.com).

placentation have started to shed light on the genes and gene networks that are involved in normal murine placentation (Cross et al., 1994; Rinkenberger et al., 1997; Cross, 2000; Hemberger and Cross, 2001; Rossant and Cross, 2001). These mouse models frequently exhibit ablation of a specific placental cell type, such as the spongiotrophoblast (Guillemot et al., 1994, 1995; Yan et al., 2001), whereas, deletion of some genes has resulted in enhanced placental growth. Placental hyperplasia for instance is caused by deletion of the genes *Esx1* (Li and Behringer, 1998), *Ipl* (Frank et al., 2002), and *Cdkn1c* (Takahashi et al., 2000). However, several placentopathies have been described that cannot be attributed to the mutation of a single gene, such as diabetes-induced placental hyperplasia in humans (Evers et al., 2003). Placental hyperplasia caused by streptozotocin-induced type II diabetes has also been demonstrated in the rat (Padmanabhan and Shafiullah, 2001). Interestingly, placental phenotypes very similar to those of diabetic rats have been found in cloned mice (Tanaka et al., 2001) and in interspecies hybrids in the rodent genera *Mus* (Zechner et al., 1996) and *Peromyscus* (Rogers and Dawson, 1970). All these placental hyperplasias exhibit several common features, such as spongiotrophoblast expansion and increased glycogen cell differentiation, even though they are caused by very different mechanisms. Thus, the *Esx1* and *Ipl* mutants are purely genetic models of placental hyperplasia caused by deletion of a single gene. In contrast to this, placental hyperplasia and the other abnormal phenotypes of cloned mice are caused entirely by disruption of epigenetic states, as cloned mice are genetically identical to their parents and the phenotypes are limited to the generation that is derived from cloning (Tamashiro et al., 2002). IHPD on the other hand has both genetic and epigenetic factors underlying the phenotype. The genetic basis of IHPD is demonstrated by strong linkage to the X chromosome (Zechner et al., 1996; Hemberger et al., 1999). Thus, placental hyperplasia is manifested in the conceptuses derived from the cross *Mus spretus* (MSP) × *Mus musculus* (MMU; SM F1), whereas hypoplasia is manifested in the reverse cross MMU × MSP (MS F1). Similarly, in the backcross MS F1 × MSP (MSS BC1) hypoplastic placentas are produced, whereas in the backcross MS F1 × MMU (MSM BC1) hyperplastic placentas are produced (Zechner et al., 1996). In these and in further backcrosses, placental dysplasia segregates with the X chromosome. Abnormal placentation was indeed observed in the AT24 congenic strain of mice in which the proximal part of the X chromosome is derived from MSP (Hemberger et al., 1999). AT24 placentas have only a mild form of hyperplasia, with weights ranging between 120 and 200 mg, yet they exhibit the morphological abnormalities of IHPD and cloned placentas, such as spongiotrophoblast expansion and increased number of glycogen cells (Hemberger et al., 1999). That epigenetic factors, apart from imprinted X inactivation in mouse trophoblast (Takagi and Sasaki, 1975; West et al., 1977), are involved in the abnormal placentation of interspecies hybrids is indicated by deregulated expression of imprinted genes (Vrana et al., 2000; Singh et al., 2004).

In a previous study, we had identified different sets of genes deregulated in IHPD and cloned and *Esx1* mutant placentas (Singh et al., 2004). Several of these genes, including *Car2*, were commonly deregulated in IHPD and cloned placentas, whereas only one gene, *Ncam1*, was common between IHPD and *Esx1* mutant placentas, albeit in opposite directions (Singh et al., 2004). Both *Car2* and *Ncam1* were upregulated in IHPD placentas. In our study, *Ncam1* expression was not consistently increased in cloned placentas; however, in another study, overexpression of *Ncam1* as well as *Car2* in cloned placentas was reported (Humpherys et al., 2002). We had also reported that *Car2* was expressed in the spongiotrophoblast and in glycogen cells of embryonic day (E) 18 MXM ((MMU × *M. macedonicus*) × MMU) and MSM placentas; however, there is no published information on the expression of *Car2* and *Ncam1* in normal mouse placentas.

Mutations for both these genes have been described previously (Lewis et al., 1988; Cremer et al., 1994). *Car2* codes for an enzyme, carbonic anhydrase 2, which has a well studied role in respiratory gas exchange (Sly et al., 1983, 1985). Normal activity of CAR2 is required for maintaining normal pH of blood and other body fluids. This enzyme is normally present in erythrocytes at a very high level. Spontaneous mutation of the *CAR2* gene in humans leads to a very variable clinical condition encompassing reduced growth, renal acidosis, osteoporosis, and reduced calcification of the bones. An *N*-ethyl-*N*-nitrosourea–induced C → T nonsense point mutation in exon 5 of the *Car2* gene in mice causes renal acidosis and runted growth (Lewis et al., 1988). During gestation, the placenta functions as the site of gas exchange for the entire conceptus. Therefore, deletion of *Car2* could be expected to cause a placental phenotype. *Ncam1* codes for a neural cell adhesion molecule and has a role in the formation of brain, especially the olfactory lobes. *Ncam1* null mice show reduced brain size with maximum reduction in the size of olfactory lobes, leading to late-onset learning defects (Cremer et al., 1994). Apart from these mild effects, the homozygous null mice for *Ncam1* are fertile. To the best of our knowledge, the functions of these two genes in normal mouse placentation have never been assessed. Consequently, this study was initiated to determine whether *Car2* and *Ncam1* have functional roles during mouse placentation as suggested by their deregulation in the two placental dysplasias with very different etiology.

We first analyzed the spatiotemporal expression patterns of *Car2* and *Ncam1* in wild-type placentas using mRNA in situ hybridization at various stages of gestation. A panel of cellular markers was used to precisely identify the various cell types that express *Car2* and *Ncam1*. In addition, we tried to determine the function of these genes in normal placentation by phenotypic analysis of *Ncam1* and *Car2* null mice; and in abnormal placentation by analysis of AT24 placentas with reduced expression of *Car2* and *Ncam1*.

RESULTS

mRNA In Situ Hybridizations

To determine the temporal and spatial expression patterns of *Car2* and

Ncam1 in normal placental development, in situ hybridization was performed on sections of wild-type placentas between gestational day (E) 8 and E18. At E8, *Car2* expression was found in the embryo, decidua, and the ectoplacental cone with no discernible expression in the yolk sac (Fig. 1A,B). At E10, very high levels of *Car2* expression were seen in the ectoplacental cone and in the parietal yolk sac, with lower levels of expression still remaining in the decidua (Fig. 1C). However, the layer of primary giant cells did not express the gene (Fig. 1D). At E12 and E14, *Car2* transcripts were primarily located in the spongiotrophoblast and in the spongiotrophoblast-derived glycogen cells; however, some foci expressing *Car2* were also present in the labyrinth (Fig. 1E,F). In situ hybridization on adjacent slides using the spongiotrophoblast-specific marker *Tpbpa* showed that a subset of *Car2*-positive cells lacked *Tpbpa* expression (Fig. 1I,J). *Car2* expression strongly decreased toward the end of the gestational period, and on E18, transcripts were found almost exclusively in the decidua (Fig. 1H). The cell types expressing *Car2* in decidua were found to be glycogen cells (Fig. 1K,L). In contrast to the situation in wild-type placentas, E18-cloned and especially IHPD placentas retained high expression of *Car2* (Fig. 1M,O). This expression of *Car2* in cloned and IHPD placentas was largely but not exclusively in the labyrinthine glycogen cells, which expressed *Tpbpa* either at very low levels or not at all (Fig. 1M,N; Fig. 1O,P; Fig. 1Q,R). In cloned placentas, *Car2* and *Tpbpa* exhibited overlapping expression only in glycogen cells situated in the decidua (Fig. 1O,P). In addition, *Car2* transcripts could be detected in chorionic plate of E18 IHPD placentas, where they were associated with fetal blood vessels (Fig. 1M). Similar results were obtained with cloned placentas (Fig. 1O). *Car2* expression was never found in the corresponding structures of wild-type placentas.

Ncam1 expression was restricted to the decidua at E8 and E10 (Fig. 2A,B). At E8, the expression was in the uterine tissue flanking the ectoplacental cone and surrounding the primary giant trophoblasts (Fig. 2A). At E10, only the region around primary giant cells retained expression of *Ncam1* (Fig. 2B). At E12, very low levels of *Ncam1* transcripts were located in the maternal cells in the decidua, in a subset of spongiotrophoblast cells, and in the chorionic plate (Fig. 2C). At E14 and E16, *Ncam1* was expressed primarily in glycogen cells in the spongiotrophoblast and chorionic plate (Fig. 2D–J). Unexpectedly, in E18 IHPD placentas, *Ncam1* transcripts were detected at ectopic sites, predominantly in labyrinth and maternal decidua (Fig. 2K). In E18 cloned placentas, ectopic expression was also detected in the labyrinth; however, at relatively low levels compared with IHPD placentas (Fig. 2L). The ectopic expression of *Ncam1* in E18 IHPD placentas was mainly harbored in clusters of cells, present in the labyrinth (Fig. 2M,N). Many such *Ncam1*-expressing foci were concentrated near the chorionic plate region (Fig. 2K,M). Whereas a diffuse expression of *Ncam1* was present throughout the labyrinth, the spongiotrophoblast of IHPD placentas appeared to be devoid of *Ncam1* transcripts (Fig. 2O). In both IHPD and cloned placentas, *Ncam1* transcripts were not present in glycogen cells situated in spongiotrophoblast and labyrinth (Fig. 2N). However, the very weak *Ncam1* expression in the decidua seemed to be present also in glycogen cells.

Placentation in *Car2*$^{-/-}$ and *Ncam1*$^{-/-}$ Mice

To determine the function of CAR2 and NCAM1 in normal placentation, heterozygous matings were performed. From *Car2*$^{-/+}$ females mated with *Car2*$^{-/+}$ males, 37 E18 fetuses were obtained. Of these, 16 (43.2%) were wild-type, 16 (43.2%) were heterozygous, and 5 (13.5%) were homozygous mutant for *Car2*. Placental weights were 103 ± 13.0, 106 ± 17.6, and 93.1 ± 11.9 mg, for wild-type, heterozygous, and homozygous mutant placentas, respectively. Student's *t*-test performed between wild-type and homozygous mutants revealed that there was no correlation between *Car2* genotype and placental weights ($P = 0.24$). From the *Ncam1*$^{-/+}$ × *Ncam1*$^{-/+}$ matings, 44 E18 fetuses were obtained. Distribution of genotypes was 15 (34.09%) wild-type, 25 (56.81%) heterozygous, and 4 (9.09%) homozygous mutants. Placental weights were, in the same order, 89.2 ± 10.2, 91.5 ± 11.2, and 98.5 ± 2.30. A Student's *t*-test performed between wild-type and homozygous mutants showed no significant difference ($P = 0.94$). Thus, neither *Car2* nor *Ncam1* deletion had significant effects on placental weight, even though homozygous mutants were underrepresented in both the *Car2* and *Ncam1* matings. Previous studies had shown that, in some congenic models of IHPD, placental overgrowth can be lost but subphenotypes such as spongiotrophoblast expansion may be retained (Hemberger et al., 1999). We, therefore, performed morphometric measurements of the relative areas occupied by decidua, spongiotrophoblast, including glycogen cells and giant cells, and labyrinth in the wild-type and mutant placentas. Averaged data from two sections from different regions of two placentas revealed that there was no significant difference in the composition of homozygous mutant versus wild-type placentas for either of the two the genes (not shown). Counting of giant cell numbers and visual assessment of the area occupied by the glycogen cells revealed no discernible difference between the wild-type and mutant placentas (not shown).

Expression of Functional Counterpart Genes

It is known that CAR1 and CAR3 are functionally redundant to CAR2 in *Car2* null mice (Lewis et al., 1988). The same is true for NCAM2, which can compensate for NCAM1 in *Ncam1* null mice (Alenius and Bohm, 2003). To see if *Car1*, *Car3*, and *Ncam2* are expressed in placentas, and thus could be responsible for the normal phenotypes of *Car2* and *Ncam1* mutant placentas, semiquantitative reverse transcription polymerase chain reactions (sqRT-PCRs) were performed for *Car1* and *Car3* in wild-type and *Car2* mutant placentas and for *Ncam2* in wild-type and *Ncam1* mutant placentas. All placentas were at E18 of gestation. This analysis detected high levels of

Car3 and *Ncam2* transcript levels (Fig. 3E), whereas expression of *Car1* was barely detectable after 30 cycles of PCR amplification (not shown). sqRT-PCRs detected no consistent expression differences, for both *Car3* and *Ncam2*, between wild-type and mutant placentas (Fig. 3E). Compensation for the loss of CAR2 and NCAM1 by CAR3 and NCAM2, respectively, requires spatially overlapping expression. In situ hybridization for *Car3* and *Ncam2* on E18 $Car2^{-/-}$ and $Ncam1^{-/-}$ placentas, respectively, showed that both genes are expressed in spongiotrophoblast (Figs. 1S,T, 2P,Q) and, thus, can potentially take over the functions of *Car2* and *Ncam1*, respectively.

AT24 Expression Analysis

In hyperplastic IHPD and cloned placentas, both *Car2* and *Ncam1* are overexpressed. The lack of any discernible phenotype in $Car2^{-/-}$ and $Ncam1^{-/-}$ placentas, which can probably be explained by expression of *Car3* and *Ncam2*, therefore, does not exclude the possibility that overexpression of either of the genes is causally involved in the generation of the phenotypes of cloned and IHPD placentas. This question could be addressed by analysis of transgenic mice that express *Car2* or *Ncam1* in a strictly tissue-specific manner. Alternatively, reducing the expression levels of either of these genes in IHPD placentas to approximately normal levels should be able to rescue at least some of the abnormal phenotypes in case *Car2* or *Ncam1* overexpression is a cause and not just a consequence of these phenotypes.

To determine whether placental hyperplasia could be rescued by decreasing transcript levels of *Car2* and *Ncam1*, $Car2^{+/-}$ and $Ncam1^{+/-}$ males were mated with AT24/AT24 homozygous females. As mentioned above, the AT24 strain is congenic for MSP-derived 20 cM of proximal X chromosome in a B6 inbred MMU background. This is sufficient to cause a milder form of placental hyperplasia (Hemberger et al., 1999). The use of the AT24 strain allowed us to avoid the use of F1 females, in F1 × $Car2^{+/-}$ or F1 × $Ncam1^{+/-}$ matings, which would have complicated considerably the analysis of placental phenotypes due to recombination during meiosis in F1 females. On the other hand, AT24 placentas exhibit a milder form of hyperplasia compared with MSM placentas, and gene expression had to be tested before AT24 could be used in the rescue study. Both, microarray hybridization and real-time quantitative reverse transcription polymerase chain reaction (qRT-PCR) were applied to assess gene expression in AT24 placentas.

Two E18 AT24 and two sex- and age-matched wild-type placentas were used for microarray hybridization. At a threshold of M value ≤ -0.5 and $\geq +0.5$, 312 expressed sequence tags (ESTs) were found to be deregulated, of which, 199 were upregulated and 113 were downregulated in the AT24 placentas compared with the wild-type controls. A list of differentially expressed ESTs is given in Supplementary Table S1 (which can be viewed at http://www.interscience.wiley.com/jpages/1058-8388/suppmat). Chromosomal localization analysis of deregulated ESTs revealed no preferential deregulation on any specific chromosome. However, the nine deregulated ESTs that map to the X chromosome (*Slc25a5*, *Calb3*, *Shbkbp1*, *F8a*, *Irak1*, *Cetn2*, *Alas2*, A430107J06Rik and 1300002C13Rik) were unevenly spread out on the chromosome. Five of these (*Slc25a5*, *Sh3kbp1*, *F8a*, *Irak1*, and *Cetn2*) are located in the region of 12.0 cM to 37 cM, which approximately is the MSP-derived region in the AT24 mice. Thirteen ESTs identified in the AT24 dataset were common to those identified deregulated in IHPD hyperplastic placentas in the previous study, when applying a threshold of 1.5-fold. These commonly deregulated ESTs represented the following genes: *Sh3kbp1*, *Plac8*, *Rap1ga1*, *Abcb7*, *Edg2*, *Dnaja3*, *Smpd1*, *Ralb*, *Igfbp4*, *Cops7a*, *Fnta*, and 9130413I22Rik55. As a large number of genes that had exhibited altered expression in our previous study, including *Car2* and *Ncam1*, are not present on the Mouse 15K (M15K) microarrays used in this study, we performed qRT-PCR for several of these genes to ascertain their expression in AT24 placentas (Fig. 3A).

Verification of Microarray Data and RT-PCR

Three littermate E18 AT24 placentas and 2 E18 B6 placentas were used for qRT-PCR and sqRT-PCR analyses. Placental weights were 151 mg and 163 mg (AT24 males), 128 mg (AT24 female), 102 mg (B6 male), and 104 mg (B6 female). To test the quality of the current microarray hybridization, qRT-PCR was performed for *Dnmt3b*, *Slc25a5*, *F8a*, *Irak1*, and *Cetn2*. For this panel of genes, the qRT-PCR results were in agreement with the microarray results (Fig. 3B,C). In addition, we tested the performance of some genes with altered expression in IHPD placentas (Singh et al., 2004). Of these genes, *Sh3kbp1*, *Plac8*, and *Ramp2* were present on the M15K microarrays, whereas *Car2*, *Ncam1*, *Dcn*, and *Gatm* were not. *Sh3kbp1* was analyzed using sqRT-PCR only (Fig. 3D), whereas for the other genes, qRT-PCR was applied. *Plac8* was measured using both techniques (Fig. 3B–D). All these genes exhibited discernible expression differences in AT24 placentas compared with the wild-type placentas. *Ramp2*, however, had not shown significant variation in the AT24 microarray hybridizations, whereas *Sh3kbp1* exhibited striking overexpression in AT24 placentas compared with the wild-type placentas (Fig. 3D).

Effects of Reduced *Car2* and *Ncam1* Transcript Levels on Phenotype of AT24 Placentas

From the cross AT24/AT24 × $Car2^{-/+}$, two litters consisting of 11 pups were obtained. Placental weights were 160 ± 14.1 for $Car2^{+/+}$ (n = 3; 2 males, 1 female) and 163 ± 28.1 for $Car2^{+/-}$ (n = 8; 5 male, 3 female). Thus placental weights of $Car2^{+/+}$ and $Car2^{+/-}$ are not significantly different.

Similar results were provided by the AT24/AT24 × $Ncam1^{-/+}$ matings. A total of 11 placentas derived from two matings were analyzed, 6 $Ncam1^{+/+}$ (3 male, 3 female) with a mean weight of 140 ± 18.7 mg and 5 $Ncam1^{+/-}$ (4 male, 1 female) with a mean weight of 153 ± 7.51 mg. Again, heterozygosity for the *Ncam1* null allele had no influence on the weight of

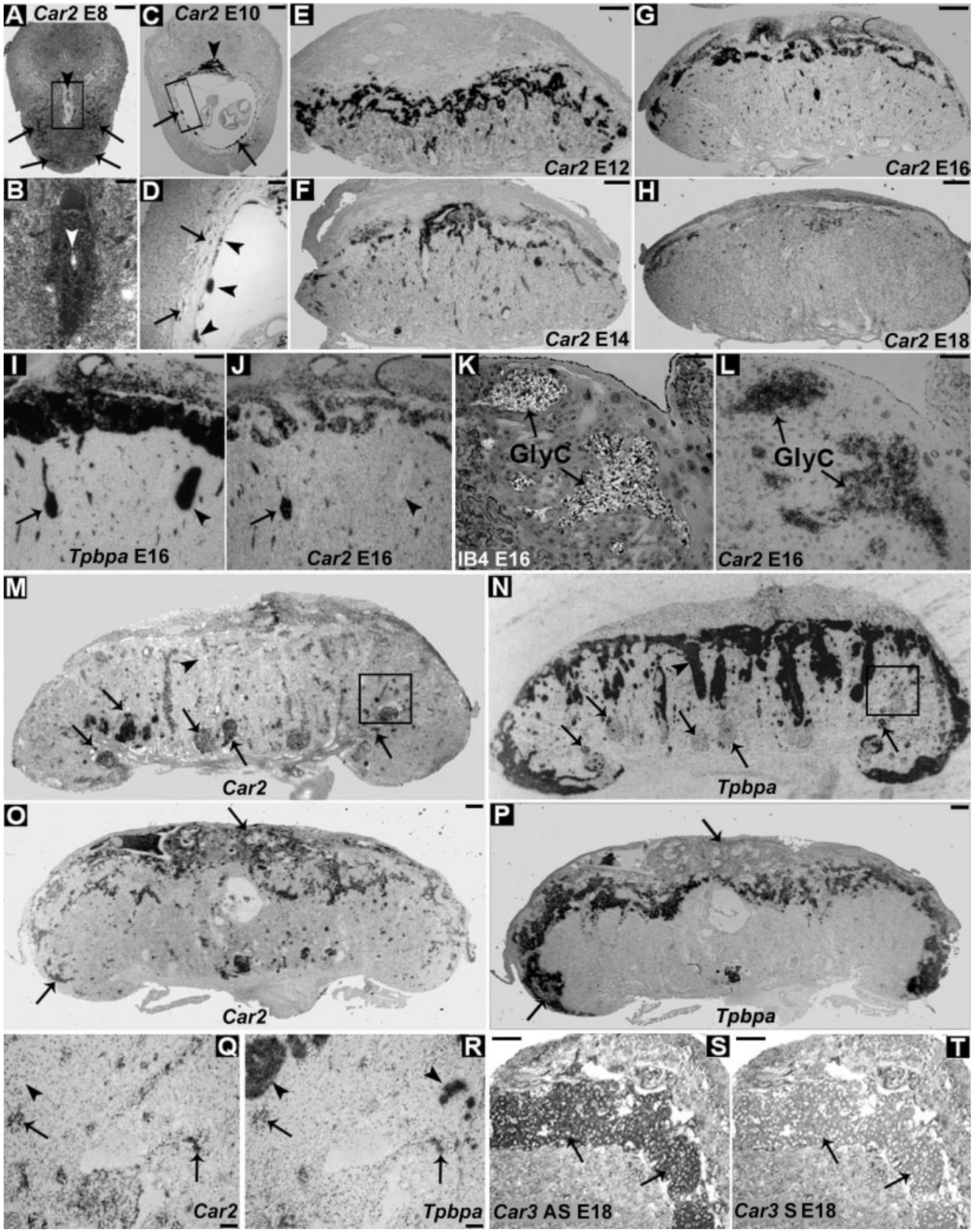
A Car2 E8
C Car2 E10
E Car2 E12
G Car2 E16
B
D
F Car2 E14
H Car2 E18
I Tpbpa E16
J Car2 E16
K GlyC IB4 E16
L GlyC Car2 E16
M Car2
N Tpbpa
O Car2
P Tpbpa
Q Car2
R Tpbpa
S Car3 AS E18
T Car3 S E18

Fig. 1.

AT24/$^{+}$ placentas. Comparative morphometric analysis, performed as described above, on isolectin B4-stained sections of AT24 heterozygous placentas, which were *Car2*$^{+/+}$ and *Car2*$^{-/+}$ and *Ncam1*$^{+/+}$ and *Ncam1*$^{+/-}$, provided no evidence for a rescue of the AT24 phenotype (not shown). Finally, to determine whether heterozygosity for *Ncam1* did actually cause decreased mRNA levels, we performed qRT-PCR analysis on placentas derived from one AT24/AT24 × *Ncam1*$^{-/+}$ mating. This analysis clearly showed that AT24/$^{+}$; Ncam1$^{+/-}$ placentas do have reduced *Ncam1* transcript levels compared with AT24/$^{+}$; *Ncam1*$^{+/+}$ placentas (Fig. 4).

DISCUSSION

We had earlier identified a large number of genes that exhibit altered expression in three models of placental hyperplasia in the mouse: cloning by somatic cell nuclear transfer (Singh et al., 2004), interspecific hybridization, and mutation of the transcription factor-encoding gene *Esx1*. However, it is a major challenge to identify the role of any of those genes in placental hyperplasia; that is, whether deregulation of a gene is just a consequence of altered phenotype, such as trophoblast expansion, or whether it is causative in producing the phenotype. In the present study, we focused on two genes, *Car2* and *Ncam1*, both of which are overexpressed in IHPD and in cloned placentas. Importantly, however, these genes were not upregulated in *Esx1* null placentas, which exhibit a very similar phenotype compared with IHPD and cloned placentas (Li and Behringer, 1998). Thus, it was reasonable to assume that the upregulation observed in IHPD and cloned placentas was not just a result of changed tissue composition, that is, spongiotrophoblast expansion at the expense of labyrinth. In this case, the assumption was even valid, as both *Car2* and *Ncam1* exhibited ectopic expression sites in hyperplastic IHPD and cloned placentas compared with age-matched controls.

Our results with mRNA in situ hybridization show that both *Car2* and *Ncam1* are expressed in normal placentas during development in a very well-defined spatiotemporal manner. Of interest, toward the end of gestation, transcripts of both genes are found predominantly in the spongiotrophoblast-derived glycogen cells. These are the only known trophoblast cells that invade into the maternal deciduas beyond the zone of secondary giant cell invasion (Redline et al., 1993). It has been argued that glycogen cells could potentially modify feto-maternal interactions, as they are closely associated with maternal blood sinuses and spongiotrophoblasts and are known to express growth factors such as insulin-like growth factor-2 and inducers of placental lactogen (Redline et al., 1993; Farnsworth and Talamantes, 1998). There is also some evidence that, in paternal isodisomy 12, shallow invasion of glycogen cells into the decidua is associated with failure of the wall of the central maternal artery to undergo a transformation associated with loss of smooth muscle contractibility and extensive deposition of acellular material (Georgiades et al., 2001). Interestingly, compromised invasion of cytotrophoblasts, which may be the human analogues of glycogen cells, has been suggested to cause failure of arterial wall transformation in human pregnancy (Han and Carter, 2000).

Car2 encodes a cytosolic zinc metalloenzyme and belongs to a large family of genes of great physiological importance. As catalysts of the reversible hydration of carbon dioxide, these enzymes participate in a variety of biological processes, including respiration, calcification, acid–base balance, and bone resorption. Expression of carbonic anhydrases in the placenta is believed to primarily serve in gas exchange and transport (Mühlhauser et al., 1994). Histochemical analysis has demonstrated that, in the rat placenta, enzyme activity is located in the syncytiotrophoblast layers of the labyrinth, in close proximity to the maternal blood spaces; however, no mention of carbonic anhydrase activity in the spongiotrophoblast or glycogen cells was made in this work nor was it shown which carbonic anhydrase isozymes are active in the labyrinth (Ridderstrale et al., 1997). However, in a later study, expression of the membrane-bound *Car4* was assessed in some detail in the murine placenta (Rosen et al., 2001). This immunohistochemical study detected the presence of CAR4 protein in labyrinthine trophoblast, that is, in the location where enzyme activity had been detected (Ridderstrale et al.,

Fig. 1. Spatiotemporal in situ expression profile of *Car2* in early wild-type conceptuses, late wild-type, interspecies hybridization (IHPD), and cloned placentas and in situ expression of *Car3* in *Car2* null placentas. **A:** At embryonic day (E) 8; arrows show expression in the decidua, and the arrowhead shows the expression in the embryo. **B:** Darkfield image of the rectangle encompassed region in A at higher magnification; the arrowhead points toward expression in the embryo. **C:** At E10; the arrowhead points at the expression in the ectoplacental cone, and arrows show expression in the parietal yolk sac. **D:** High-magnification image of the rectangle encompassed region in C; arrowheads show expression in the yolk sac, and arrows point toward primary giant cells devoid of expression. **E:** At E12. **F:** At E14. **G:** At E16. **H:** At E18. From E12 to E18, progressive loss of expression in the spongiotrophoblast and gain of expression in the decidua can be seen. **I:** *Tpbpa* hybridization on E16 placenta. **J:** *Car2* hybridization on a section adjacent to I; the arrow shows area of overlapping expression, and the arrowhead shows area of nonoverlapping expression. **K:** Isolectin B4 staining on E16 placenta; arrows indicate pegs of glycogen cells. **L:** *Car2* expression on section adjacent to K; arrows show that cells expressing *Car2* are actually glycogen cells. **M:** *Car2* expression in E18 IHPD MXM placenta weighing 404 mg. **N:** *Tpbpa* expression on a section adjacent to K; arrows show regions of overlapping expression, and the arrowhead shows regions of nonoverlapping expression. The areas surrounded by the rectangles in M and N have been magnified in Q and R, respectively. **O:** *Car2* expression in E18 cloned placenta weighing 230 mg. **P:** *Tpbpa* expression on a section adjacent to O; arrows show regions of overlapping expression. **Q,R:** High-magnification images of *Car2* and *Tpbpa* hybridizations, respectively, on adjacent sections of E18 IHPD MXM placenta weighing 511 mg; arrows show areas of overlapping expression, and arrowheads show areas of nonoverlapping expression. **S,T:** Nonradioactive in situ expression analysis for *Car3* in E18 *Car2*$^{-/-}$ placentas; arrows show that the expression of *Car3* is in the spongiotrophoblast of *Car2*$^{-/-}$ placentas; T shows hybridization with a sense probe on a section adjacent to S. GlyC, glycogen cells; IB4, Isolectin B4; S, sense probe; AS, antisense probe. Scale bar = 500 μm in A,C,E–H,M–P, 125 μm in I,J,S,T, 100 μm in B,D, 50 μm in K,L, 65 μm in Q,R.

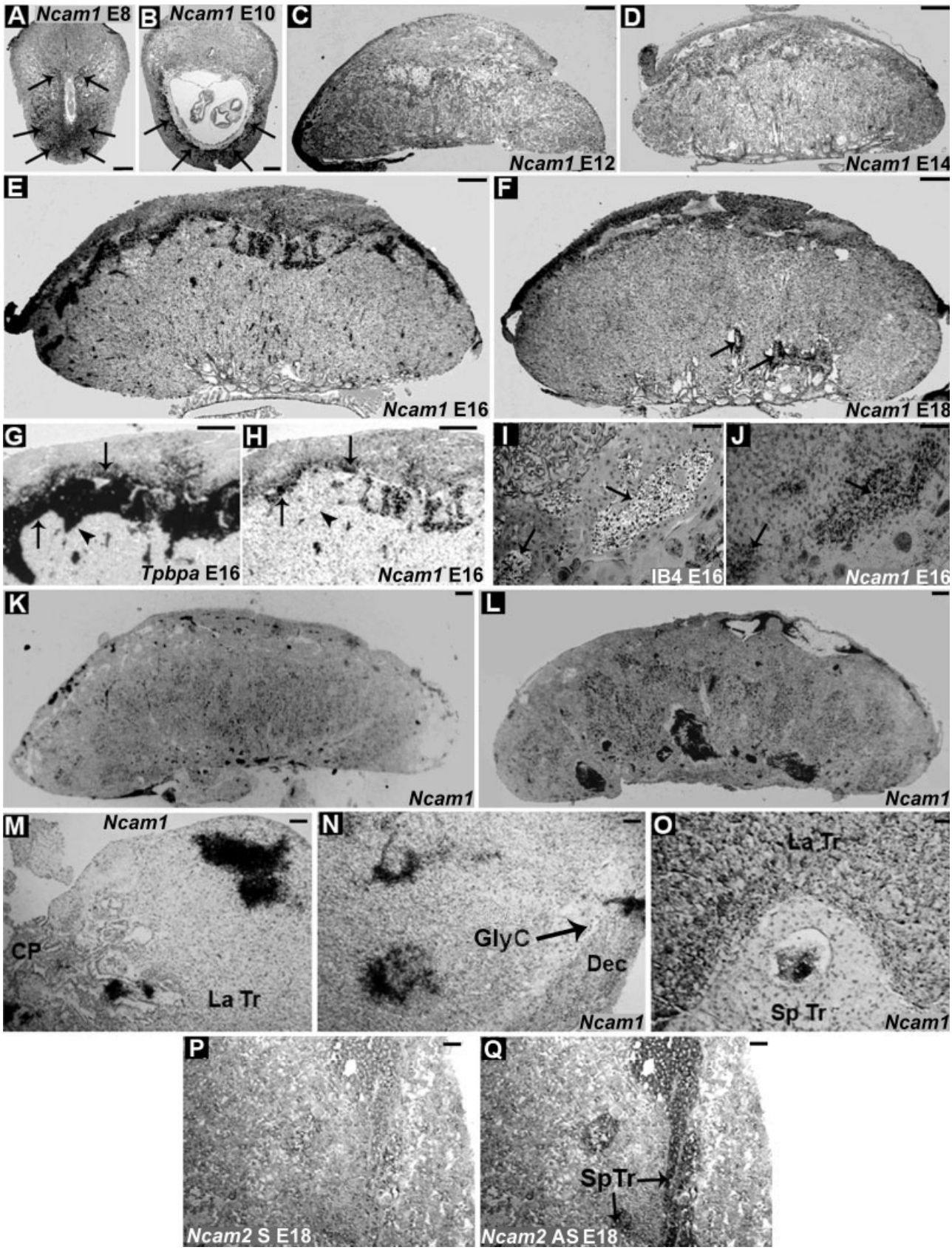
A Ncam1 E8
B Ncam1 E10
C Ncam1 E12
D Ncam1 E14
E Ncam1 E16
F Ncam1 E18
G Tpbpa E16
H Ncam1 E16
I IB4 E16
J Ncam1 E16
K Ncam1
L Ncam1
M Ncam1
CP
La Tr
N GlyC
Dec
Ncam1
O La Tr
Sp Tr
Ncam1
P Ncam2 S E18
Q SpTr
Ncam2 AS E18

Fig. 2.

1997); however, spongiotrophoblast and glycogen cells were clearly negative for CAR4. Thus, this study is the first to describe expression by mRNA in situ hybridization of *Car2*, and *Car3*, in the mouse placenta. It is unclear, what function CAR2 and CAR3 could have in spongiotrophoblast and glycogen cells, which are not very well located to significantly contribute to CO_2 exchange. Unfortunately, deletion of *Car2* alone did not result in any phenotype detectable by the methods applied by us, which was most likely caused by CAR3 taking over the functions of CAR2. Thus, the question as to the function of CAR2 activity in spongiotrophoblast and glycogen cells can at present not be answered.

The same is true for *Ncam1*, which encodes a cell adhesion molecule with multiple roles in brain development (Edelman and Jones, 1997), neuronal pathfinding (Hanson and Landmesser, 2004), and also in tumor metastasis (Christofori, 2003). Accordingly, mice with homozygous mutation of the *Ncam1* gene show mostly neural phenotypes, such as impairment in the Morris water maze test, reduced brain and olfactory bulb size, hypoplastic corticospinal tract, abnormally distributed anterior pituitary cell types, and morphological and functional defects of neuromuscular junctions (Cremer et al., 1994). High expression of *Ncam1* has been described in the human placenta, where the gene is strongly expressed in the endovascular trophoblast (Burrows et al., 1994). It was argued that expression of NCAM1 and other cell adhesion molecules is relevant for vascular invasion by trophoblast by permitting interactions between endovascular trophoblast and decidual endothelial cells (Burrows et al., 1994). The expression of *Ncam1* in the mouse placenta has not been described previously nor is there any information available on the function of NCAM1 in this organ. Expression of *Ncam1* in glycogen cells, an invasive trophoblast cell type in the mouse placenta, suggests that NCAM1 may serve a similar function as NCAM in the human placenta, that is, to permit interactions between the trophoblasts and the decidual cells. Unfortunately, the lack of any phenotype in the $Ncam1^{-/-}$ placentas, probably a result of *Ncam2* expression, allows no final statement regarding the role of NCAM1 in the mouse placenta.

Whereas the absence of obvious phenotypes associated with ablation of CAR2 or NCAM1 may be explained by redundancy, lack of rescue of the AT24 phenotype in the AT24/AT24 $\times$ $Car2^{+/-}$ and AT24/AT24 $\times$ $Ncam1^{+/-}$ matings strongly indicates that the upregulation of the two genes in AT24 placentas and, thus, by extension, in cloned and IHPD placentas, does not contribute significantly to their phenotypes. This conclusion is obvious in the case of the AT24 placentas; however, there is good evidence that the same is true for IHPD and perhaps cloned placentas. First, we have shown by both microarray hybridization and qRT-PCR that, where gene expression is concerned, the AT24 placentas provide an excellent model for IHPD. This finding was expected, as IHPD and AT24 share a MSP-derived region on the X chromosome, which alone is sufficient to induce placental hyperplasia (Zechner et al., 1996; Hemberger et al., 1999) and, thus, at least in part the genes that cause placental overgrowth. For *Ncam1*, we could also show that its transcript levels are indeed reduced in AT24/$^{+}$; $Ncam1^{+/-}$ placentas by approximately 50%. As *Ncam1* is upregulated by a factor of roughly twofold in both AT24 and IHPD placentas (Singh et al., 2004), this finding suggests that *Ncam1* transcript levels were decreased to approximately wild-type levels in the AT24/$^{+}$; $Ncam1^{+/-}$ placentas. If *Ncam1* was upstream in the cascade of genes deregulated in placental hyperplasia, a rescue of the AT24 phenotype or one of the subphenotypes such as spongiotrophoblast expansion or increased glycogen cell differentiation should have been visible. The same most likely also applies to *Car2*, even though we did not formally show that levels of wild-type and functional transcripts are downregulated in the AT24/$^{+}$; $Car2^{+/-}$ placentas.

Apart from the studies on *Car2* and *Ncam1* expression and function in the mouse placenta, we also show results of global gene expression analysis in an additional model of placental hyperplasia, the AT24 congenic strain. This analysis has identified several interesting genes. For instance, one of the two imprinted genes with altered expression, *Grb10*, codes for a major determinant of placental growth and function (Charalambous et al., 2003). Deregulation of *Dnmt3b*, a gene encoding a de novo methyltransferase, potentially could lead to altered epigenetic states and to imprinting defects in AT24 placentas. Of interest, this gene was expressed at normal levels in backcross 1 interspecies placentas. It may also be relevant that five genes with altered expression, *Slc25a5*, *Sh3kbp1*, *F8a*, *Irak1*, and *Cetn2*, map to the MSP-derived region on the X chromosome in AT24 mice. However, a functional role in placentation has not been ascribed to any of these genes to date.

Fig. 2. Spatiotemporal in situ expression profile of *Ncam1* in early wild-type conceptuses, late wild-type, interspecies hybridization (IHPD), and cloned placentas and in situ expression of *Ncam2* in *Ncam1* null placentas. **A:** At embryonic day (E) 8; arrows show expression in the decidua and the region flanking the ectoplacental cone. **B:** At E10; arrows show the expression in decidua around primary giant cells. **C:** At E12. **D:** At E14. **E:** At E16. **F:** At E18, arrows show the regions of expression in chorionic plate. **G:** *Tpbpa* expression in E16 placenta. **H:** *Ncam1* expression on a section adjacent to G; arrows indicate areas of overlapping expression, and the arrowhead indicates an area of nonoverlapping expression. **I:** Isolectin B4 staining on E16 placenta; arrows indicate pegs of glycogen cells. **J:** *Ncam1* expression on a section adjacent to I; arrows show that cells expressing *Ncam1* are indeed glycogen cells. **K:** *Ncam1* expression in an E18 IHPD MXM placenta weighing 232 mg. **L:** *Ncam1* expression in an E18 cloned placenta weighing 263 mg. **M,N:** Expression of *Ncam1* in chorionic plate and labyrinth, respectively, of E18 IHPD placentas. **O:** Unlike wild-type placentas, spongiotrophoblast of IHPD placenta (MXM, 511 mg) is devoid of *Ncam1* expression. **P,Q:** Nonradioactive in situ expression analysis for *Ncam2* in E18 $Ncam1^{-/-}$ placentas shows strong expression in the spongiotrophoblast; P shows the hybridization with a sense probe on a section adjacent to Q. CP, chorionic plate; LaTr, labyrinthine trophoblasts; SpTr, spongiotrophoblast; Dec, decidua; GlyC, glycogen cells; IB4, Isolectin B4; S, sense probe; AS, antisense probe. Scale bar = 500 μm in A–F,K,L, 125 μm in G,H, 50 μm in I,J, 250 μm in M,N,P,Q, 75 μm in O.

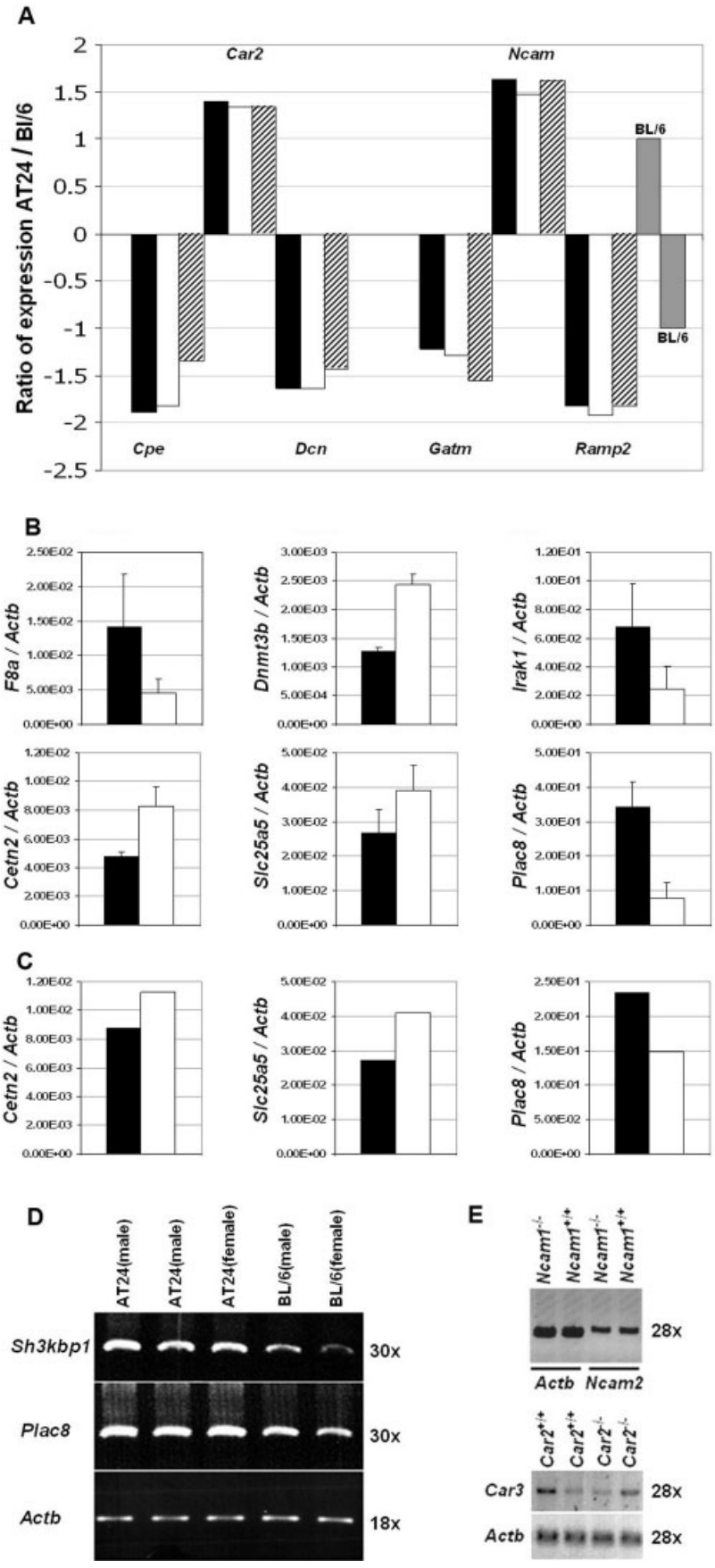

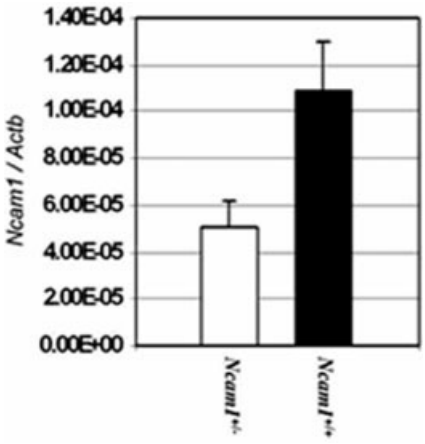

Fig. 4. Real-time quantitative reverse transcription polymerase chain reaction for *Ncam1* in littermate AT24/$^{+}$ placentas heterozygous mutant or wild-type for *Ncam1*.

EXPERIMENTAL PROCEDURES

Mice and Tissues

All experiments with mice were conducted according to the guidelines issued by Uppsala University. *Car2* mutant mice (Lewis et al., 1988) were obtained from Jackson Laboratory (Bar Harbor, ME). *Ncam1* mutant mice (Cremer et al., 1994) were kindly given to us by Prof. Carlos Ibanez, Karolinska Institute. C57BL/6J mice

Fig. 3. Real-time quantitative reverse transcription polymerase chain reaction and semiquantitative reverse transcription polymerase chain reactions (sqRT-PCRs) analysis in placental RNA samples. **A:** Genes previously identified deregulated in interspecies hybridization (IHPD) placentas and/or placentas from cloned mice; the X axis depicts the ratio of expression (normalized against *Actb*) of a particular gene in AT24 placenta to sex- and stage-matched BL/6 controls, black and white bars represent placentas from two different male conceptuses, and the striated bars represent the placenta from a female littermate pair (see text for details); the two gray bars on the extreme right with the label BL/6 indicate the ratio of 1 or −1, which suggests no change in expression in either direction. **B:** *Actb* normalized expression of genes found deregulated in male AT24 placentas compared with male BL/6 placentas. **C:** *Actb* normalized expression of various genes found deregulated in a female AT24 placenta compared with a female BL/6 placenta. **D:** sqRTPCR analysis of *Sh3kbp1* and *Plac8*, rounds of PCR mentioned at the right end of each panel. **E:** sqRTPCR for *Ncam2* and *Car3* in placentas mutant for *Ncam1* and *Car2*, respectively. The rounds of PCR are indicated at the right side of each panel.

were obtained from B&K (Stockholm, Sweden). *Car2* and *Ncam1* mutant lines were propagated in the original C57BL/6J (B6) strain background by mating heterozygous males with wild-type females. For isolation of wild-type placentas, B6 × B6 matings were used. Cloned fetuses were produced by transfer of cumulus cell nuclei of B6 × DBA/2 females as described previously (Wakayama et al., 1998). MSM placentas were produced by backcrossing F1 females with B6 males as described previously (Zechner et al., 1996; Singh et al., 2004). Pregnant females were killed by cervical dislocation at different developmental stages, with the day of vaginal plug being counted as day 1. Fetuses and placentas were weighed. Placentas were halved, and half was frozen on dry ice for RNA extraction, while the other half was fixed in Serra's fixative overnight at 4–8°C and later processed for paraffin histology. Fetal heads were frozen for DNA extraction for genotyping.

DNA Extraction and Genotyping PCRs

Genomic DNA was extracted from fetal heads by using Wizard genomic DNA extraction kit from Promega. To genotype *Ncam1* mutant mice, two different primer pairs were used in separate reactions. The wild-type allele was amplified using the primers 5′-TGCAGGGCTCATCACTGTAG-3′ and 5′-AGCAGGAGGAGCAGAGTGAG-3′, the neomycin cassette inserted in the knockout allele using the primer pair 5′-CGGCATCAGAGCAGATTGTA-3′ and 5′-GCTTCCTCTTGCAAAACCAC-3′. Reaction conditions were 94°C for 3 min (94°C for 30 sec, 55°C for 30 sec, 72°C for 45 sec) × 35, 72°C for 7 min, for the wild-type allele and 94°C for 3 min (94°C for 30 sec, 59°C for 35 sec, 72°C for 45 sec) × 35, 72°C for 7 min for the mutant allele. PCR products were resolved on 1.5% agarose gels.

Car2 mutant mice were genotyped by using PCR-based amplification followed by DNA sequencing (Supplementary Figure S1). The region of the genomic DNA harboring the C → T point mutation was amplified using the following primer pair; forward primer: 5′-GGCCTTATAACCCCTGCATT-3′ and reverse primer 5′-CATGAAAACACCATGACACCA-3′. Reaction conditions were 94°C for 3 min (94°C for 30 sec, 56°C for 30 sec, 72°C for 30 sec) × 35, 72°C for 7 min. PCR products were purified from 1% w/v agarose gel (Gel purification kit, Qiagen) and sequenced using the forward primer. Sex of fetuses was determined by a Y chromosome-specific PCR using the primer pair 5′-CATTTATGGTGTGGTCCCGTG-3′ and 5′-GTGTGCAGCTCTACTCCAG-3′. Conditions of the reaction were 94°C for 3 min (94°C for 30 sec, 60°C for 30 sec, 72°C for 40 sec) × 35, 72°C for 7 min. All genotyping PCRs were performed in PTC-100 PCR machines (MJ Research, Watertown, MA).

DNA Sequencing

DNA sequencing reaction was performed using BIG Dye Terminator Mix (Applied Biosystems) in a GeneAmp 9600 PCR machine. Precipitated and purified samples were run on the ABI PRISM automated sequencer.

mRNA In Situ Hybridization

Radioactive in situ hybridizations were performed as described previously (Krause et al., 1999). Nonradioactive in situ hybridizations were performed with slight modifications to the procedure described by Anson-Cartwright et al. (2000). *Tpbpa* hybridizations were performed using a template described before (Zechner et al., 1996). Linearized clones from the cDNA library used to make microarrays in our previous study (Singh et al., 2004) were used as in vitro transcription templates for the genes *Car2* (accession no. W41721) and *Ncam1* (accession no. AI316242). Linearization and purification of the clones was done as described earlier (Singh et al., 2004). The clone for *Ncam2* was kindly given to us by Prof. Staffan Bohm, Umeå University. For *Car3*, a 509-bp RT-PCR product was amplified using the primer pairs 5′-TGCTCCCTACTCCAAGCTGT-3′ and 5′-CCTGGCTTTATGGGTGTGTT-3′ and cloned into pGEMt vector (Promega), linearized, and used as template for in vitro transcription. The transcript using SP6 promoter gave antisense hybridization.

RNA Extraction, Microarray Hybridizations, and Data Analysis

Total RNA was extracted using Trizol reagent (Invitrogen) as per the manufacturer's instructions. Purified RNA samples (Abs 260 nm/Abs 280 nm > 1.7) were used for microarray-based expression profiling. Commercially available M15K microarrays were obtained from University Health Network (UHN; Ontario Cancer Institute, Canada). Detailed information about these microarrays is available at the following link: http://www.microarrays.ca/products/types.html. The TSA-MICROMAX kit (NEN, Perkin Elmer, Oak Brook, IL) was used for synthesizing labeled target cDNA. All steps of the protocol were performed according to the manufacturer's instructions, except that the hybridizations were done using the DIG Easy Hyb (Roche), with 1 μg of Cot1 DNA per hybridization, and Tween 20 in the TNT buffer was used at a concentration of 0.1% v/v against the kit instructions of 0.05% v/v. Dye swaps for all hybridizations were performed simutaneously.

The list of ESTs on the microarray was supplied by the UHN as a clonetracker file, and a Gene Array List (GAL) file was generated according to the format described for ScanArray Express, version 2.1.0. Hybridized and labeled microarrays were scanned immediately after washings using the ScanArray 4000 microarray scanner (Packard BioChip Technologies) and ScanArray Express (version 2.1.0) was used for generating the GPR files.

The experimental data were stored and analyzed at the microarray data storage and analysis facilities BASE and Data Ware House respectively, run by The Linnaeus Center for Bioinformatics, BMC, Uppsala University, Sweden (detailed information at http://www.lcb.uu.se, https://base.lcb.uu.se, and https://dw.lcb.uu.se). Briefly, the data in the GPR files was subjected to background subtraction and within array Print-tip Lowess normalization implemented in R. Differentially expressed genes were chosen on the basis of three criteria: higher and outstanding B value (a logarithm of odds ratio for differential expression, which takes into account the variance of

each spot across different hybridizations; Baldi and Long, 2001; Gottardo et al, 2003) compared with the majority of genes that formed the cluster in the volcano plot (see Supplementary Figure S1); M value not between −1 and +1; and such a consistent variation of these genes for duplicate spots on all the four microarrays (each EST is spotted as adjacent duplicate spots on M15K arrays). Density plots and B value volcano plot for all the hybridizations are provided in Supplementary Figure S2. Signal on control spots with 3 × standard saline citrate and Arabidopsis DNA were used to remove spots with nonspecific hybridization; however, no flags were applied. The LCB BASE and DWH facilities comply with the MIAME guidelines.

qRT-PCR and sqRT-PCR

RNA was treated with RNAse free DNAse (Promega) and reverse transcribed using M-MLV reverse transcriptase and random primers (Promega) as described earlier (Singh et al., 2004). Primers were designed using Primer3 and purchased from MWG Biotech, Germany. qRT-PCR was performed using QuantiTect SYBR green PCR mix from Qiagen. Melting curve analysis was used to ensure that a single size product was amplified, and no significant primers dimers were present. All samples were analyzed in duplicate. Reactions were run on RotorGene RG3000, Corbett Research. The ratio of the expression of each gene was calculated for each sample by normalizing the comparative quantitation values to those of *Actb*. The sequences and reaction conditions of all the primers used are provided in Supplementary Table S2. sqRT-PCRs were performed from the same cDNAs as described before (Singh et al., 2004).

Isolectin B4 Staining and Histology

Staining was performed as described by Hemberger et al. (1999). Biotinylated isolectin B4 and diaminobenzidine substrate kit were obtained from Vector Labs (Burlingame, CA) and streptavidin–horseradish peroxidase conjugate was purchased from Perkin Elmer. Morphometry was performed as described by Salas et al. (2004) using Adobe PhotoshopCS. For all morphometric measurements, isolectin B4–stained sections were used. Two sections each were used from each placenta and values were averaged for all the sections of a genotype. The area occupied by chorionic plate was excluded in the analyses.

Statistical Analysis

Student's *t*-test was performed to determine the significance of differences in placental weights between wild-type and homozygous mutants of *Car2* and *Ncam1*. The online tool available at http://www.physics.csbsju.edu/stats/t-test_bulk_form.html was used to perform the analysis. Mean and standard deviations were calculated by using MS Excel.

ACKNOWLEDGMENTS

We thank Drs. Staffan Bohm, Gustavo Paratcha, and Carlos F. Ibáñez for providing us with reagents and mouse strains. R.F. was funded by grants of the Swedish Research Council (Vetenskapsrådet) and the Wallenberg Consortium North, and R.W.E. was funded by the NIH. M.H. is supported by an MRC Career Development Award.

REFERENCES

Alenius M, Bohm S. 2003. Differential function of RNCAM isoforms in precise target selection of olfactory sensory neurons. Development 130:917–927.

Anson-Cartwright L, Dawson K, Holmyard D, Fisher SJ, Lazzarini RA, Cross JC. 2000. The glial cells missing-1 protein is essential for branching morphogenesis in the chorioallantoic placenta. Nat Genet 25:311–314.

Baldi P, Long AD. 2001. A Bayesian framework for the analysis of microarray expression data: regularized t-test and statistical inferences of gene changes. Bioinformatics 17:509–519.

Burrows TD, King A, Loke YW. 1994. Expression of adhesion molecules by endovascular trophoblast and decidual endothelial cells: implications for vascular invasion during implantation. Placenta 15:21–33.

Charalambous M, Smith FM, Bennett WR, Crew TE, Mackenzie F, Ward A. 2003. Disruption of the imprinted Grb10 gene leads to disproportionate overgrowth by an Igf2-independent mechanism. Proc Natl Acad Sci U S A 100:8292–8297.

Christofori G. 2003. Changing neighbours changing behaviour: cell adhesion molecule-mediated signalling during tumour progression. EMBO J 22:2318–2323.

Cremer H, Lange R, Christoph A, Plomann M, Vopper G, Roes J, Brown R, Baldwin S, Kraemer P, Scheff S, Barthels D, Rajewsky K, Wille W. 1994. Inactivation of the N-CAM gene in mice results in size reduction of the olfactory bulb and deficits in spatial learning. Nature 367:455–459.

Cross JC. 2000. Genetic insights into trophoblast differentiation and placental morphogenesis. Semin Cell Dev Biol 11: 105–113.

Cross JC, Werb Z, Fisher SJ. 1994. Implantation and the placenta: key pieces of the development puzzle. Science 266:1508–1518.

Edelman GM, Jones FS. 1997. Gene regulation of cell adhesion molecules in neural morphogenesis. Acta Paediatr Suppl 422:12–19.

Evers IM, Nikkels PGJ, Sikkema JM, Visser GHA. 2003. Placental pathology in women with type 1 diabetes and in a control group with normal and large-for-gestational-age infants. Placenta 24:819–825.

Farnsworth RL, Talamantes F. 1998. Calcyclin in the mouse decidua: expression and effects on placental lactogen secretion. Biol Reprod 59:546–552.

Frank D, Fortino W, Clark L, Musalo R, Wang W, Saxena A, Li CM, Reik W, Ludwig T, Tycko B. 2002. Placental overgrowth in mice lacking the imprinted gene Ipl. Proc Natl Acad Sci U S A 99: 7490–7495.

Georgidaes P, Watkins M, Burton GJ, Ferguson-Smith AC. 2001. Roles for genomic imprinting and the zygotic genome in placental development. Proc Natl Acad Sci U S A 98:4522–4527.

Gottardo R, Pannucci JA, Kuske CR, Brettin T. 2003. Statistical analysis of microarray data: a Bayesian approach. Biostatistics 4:597–620.

Guillemot F, Nagy A, Auerbach A, Rossant J, Joyner AL. 1994. Essential role of Mash-2 in extraembryonic development. Nature 371:333–336.

Guillemot F, Caspary T, Tilghman SM, Copeland NG, Gilbert DJ, Jenkins NA, Anderson DJ, Joyner AL, Rossant J, Nagy A. 1995. Genomic imprinting of Mash2 a mouse gene required for trophoblast development. Nat Genet 9:235–242.

Han VK, Carter AM. 2000. Spatial and temporal patterns of expression of messenger RNA for insulin-like growth factors and their binding proteins in the placenta of man and laboratory animals. Placenta 21:289–305.

Hanson MG, Landmesser LT. 2004. Normal patterns of spontaneous activity are required for correct motor axon guidance and the expression of specific guidance molecules. Neuron 43:687–701.

Hemberger M, Cross JC. 2001. Genes governing placental development. Trends Endocrinol Metab 12:162–168.

Hemberger MC, Pearsall RS, Zechner U, Orth A, Otto S, Ruschendorf F, Fundele

R, Elliott R. 1999. Genetic dissection of X-linked interspecific hybrid placental dysplasia in congenic mouse strains. Genetics 153:383–390.

Humpherys D, Eggan K, Akutsu H, Friedman A, Hochedlinger K, Yanagimachi R, Lander ES, Golub TR, Jaenisch R. 2002. Abnormal gene expression in cloned mice derived from embryonic stem cell and cumulus cell nuclei. Proc Natl Acad Sci U S A 99:12889–12894.

Krause R, Hemberger M, Himmelbauer H, Kalscheuer V, Fundele RH. 1999. Identification and characterization of G90 a novel mouse RNA that lacks an extensive open reading frame. Gene 232:35–42.

Lewis SE, Erickson RP, Barnett LB, Venta PJ, Tashian RE. 1988. N-ethyl-N-nitrosourea-induced null mutation at the mouse Car-2 locus: an animal model for human carbonic anhydrase II deficiency syndrome. Proc Natl Acad Sci U S A 85: 1962–1966.

Li Y, Behringer RR. 1998. *Esx1* is an X-chromosome-imprinted regulator of placental development and fetal growth. Nat Genet 20:309–311.

Mühlhauser J, Crescimanno C, Rajaniemi H, Parkkila S, Milanov AP, Castellucci M, Kaufmann P. 1994. Immunohistochemistry of carbonic anhydrase in human placenta and fetal membranes. Histochemistry 101:91–98.

Padmanabhan R, Shafiullah M. 2001. Intrauterine growth retardation in experimental diabetes: possible role of the placenta. Arch Physiol Biochem 109:260–271.

Redline RW, Chernicky CL, Tan HQ, Ilan J, Ilan J. 1993. Differential expression of insulin-like growth factor-II in specific regions of the late (post day 9.5) murine placenta. Mol Reprod Dev 36:121–129.

Ridderstrale Y, Persson E, Dantzer V, Leiser R. 1997. Carbonic anhydrase activity in different placenta types: a comparative study of pig horse cow mink rat and human. Microsc Res Tech 38:115–124.

Rinkenberger JL, Cross JC, Werb Z. 1997. Molecular genetics of implantation in the mouse. Dev Genet 2:6–20.

Rogers JF, Dawson WD. 1970. Foetal and placental size in a Peromyscus species cross. J Reprod Fertil 21:255–262.

Rossant J, Cross JC. 2001. Placental development: lessons from mouse mutants. Nat Rev Genet 2:538–548.

Rosen O, Suarez C, Schuster VL, Brion LP. 2001. Expression of carbonic anhydrase IV in mouse placenta. Am J Physiol Regul Integr Comp Physiol 280:365–375.

Salas M, John R, Saxena A, Barton S, Frank D, Fitzpatrick G, Higgins MJ, Tycko B. 2004. Placental growth retardation due to loss of imprinting of Phlda2. Mech Dev 121:1199–1210.

Singh U, Fohn LE, Wakayama T, Ohgane J, Steinhoff C, Lipkowitz B, Schulz R, Orth A, Ropers HH, Behringer RR, Tanaka S, Shiota K, Yanagimachi R, Nuber UA, Fundele R. 2004. Different molecular mechanisms underlie placental overgrowth phenotypes caused by interspecies hybridization cloning and Esx1 mutation. Dev Dyn 230:149–164.

Sly WS, Hewett-Emmett D, Whyte MP, Yu YS, Tashian RE. 1983. Carbonic anhydrase II deficiency identified as the primary defect in the autosomal recessive syndrome of osteopetrosis with renal tubular acidosis and cerebral calcification. Proc Natl Acad Sci U S A 80:2752–2756.

Sly WS, Whyte MP, Sundaram V, Tashian RE, Hewett-Emmett D, Guibaud P, Vainsel M, Baluarte HJ, Gruskin A, Al-Mosawi M, Sakati N, Ohlsson A. 1985. Carbonic anhydrase II deficiency in 12 families with the autosomal recessive syndrome of osteopetrosis with renal tubular acidosis and cerebral calcification. N Engl J Med 313:139–145.

Takagi N, Sasaki M. 1975. Preferential inactivation of the paternally derived X chromosome in the extraembryonic membranes of the mouse. Nature 256: 640–642.

Takahashi K, Kobayashi T, Kanayama N. 2000. p57(Kip2) regulates the proper development of labyrinthine and spongiotrophoblasts. Mol Hum Reprod 6:1019–1025.

Tamashiro KL, Wakayama T, Akutsu H, Yamazaki Y, Lachey JL, Wortman MD, Seeley RJ, D'Alessio DA, Woods SC, Yanagimachi R, Sakai RR. 2002. Cloned mice have an obese phenotype not transmitted to their offspring. Nat Med 8:262–267.

Tanaka S, Oda M, Toyoshima Y, Wakayama T, Tanaka M, Yoshida N, Hattori N, Ohgane J, Yanagimachi R, Shiota K. 2001. Placentomegaly in cloned mouse concepti caused by expansion of the spongiotrophoblast layer. Biol Reprod 65:1813–1821.

Vrana PB, Fossella JA, Matteson P, del Rio T, O'Neill MJ, Tilghman SM. 2000. Genetic and epigenetic incompatibilities underlie hybrid dysgenesis in Peromyscus. Nat Genet 25:120–124.

Wakayama T, Perry ACF, Zuccotti M, Yanagimachi R. 1998. Full term development of mice from enucleated oocytes injected with cumulus cell nuclei. Nature 394:369–374.

West JD, Frels WI, Chapman VM, Papaioannou VE. 1977. Preferential expression of the maternally derived X chromosome in the mouse yolk sac. Cell 12:873–882.

Yan J, Tanaka S, Oda M, Makino T, Ohgane J, Shiota K. 2001. Retinoic acid promotes differentiation of trophoblast stem cells to a giant cell fate. Dev Biol 235:422–432.

Zechner U, Reule M, Orth A, Bonhomme F, Strack B, Guenet, Hameister H, Fundele R. 1996. An X-chromosome linked locus contributes to abnormal placental development in mouse interspecific hybrid. Nat Genet 12:398–403.